Author version: *Pure Appl. Geophys., vol.173(4); 2016; 1305-1316*

Estimation of Sea Surface Temperature (SST) using Marine Seismic Data

Satish Kumar Sinha*
Rajiv Gandhi Institute of Petroleum Technology, Rae Bareli, India

Pawan Dewangan
CSIR-National Institute of Oceanography, Goa, India

Kalachand Sain
CSIR-National Geophysical Research Institute, Hyderabad, India

Abbreviated Title: Sea surface temperature using marine seismic

*Corresponding author address: Satish Kumar Sinha, Rajiv Gandhi Institute of Petroleum Technology, Rae Bareli, Uttar Pradesh, India 229316.
E-mail: ssinha@rgipt.ac.in , satish.sinha@gmail.com

ABSTRACT

Not much attention is given to direct wave arrivals in marine seismic data that are acquired for petroleum exploration and prospecting. These direct arrivals are usually muted out in routine seismic data processing. In the present study, we process these direct arrivals to accurately estimate soundspeed in near surface seawater and invert for sea surface temperature (SST). The established empirical equation describing the relationships among temperature, salinity, pressure and soundspeed is used for the inversion. We also discuss processing techniques, such as first-break picking and cross-correlation for the estimation of soundspeed, that are well known among petroleum-industry geophysicists. The accuracy of the methods is directly linked to the data quality and signal processing. The novelty in our approach is in the data conditioning, which consists essentially of spectral balancing based on a wavelet transform that compensates for spherical spreading and increases the signal-to-noise (S/N) ratio. The 2D seismic data used in this paper are from the offshore Krishna-Godavari Basin east of India. We observe a significantly higher soundspeed of 1545 m/s for near surface water than the commonly used value of ~1500 m/s. The estimated temperature (from velocity) is about 30^{o}C. Interestingly, the estimated temperature matches well with the temperature recorded in the CTD profile acquired in the study area during the month of May, the month corresponding to the acquisition of seismic data. Furthermore, the estimated temperatures during different times of data acquisition correlate well with the expected diurnal variation in temperature.

Keywords: *Marine Seismic; Direct Arrivals; Soundspeed; Sea Surface Temperature; Diurnal variations.*

INTRODUCTION

Properties of sound waves in oceans are governed by temperature, salinity, water composition and depth (or pressure). Several studies have reported variation of the soundspeed in seawater with different season, location, water depth as well as ocean currents [*Chen and Millero,* 1977; *Dushaw et al.*, 1993; *Grosso,* 1974; *Jones,* 1999]. To better understand ocean dynamics, researchers in the field of ocean acoustics invert for temperature and salinity from observed sound waves, whereas oceanographers measure governing parameters directly by deploying devices such as Expendable Bathythermographs (XBT), Conductivity Temperature Depth (CTD) probes, or Profile floats equipped with various types of sensors at different locations. Inference of water temperatures from acoustic propagation properties constitutes the now large subject of ocean acoustic tomography (or thermometry) [*Worcester et al.*, 1999]. *Holbrook et al.* [2003] presented acoustic images of thermohaline structure in seawater masses from seismic reflection profiles. Ocean temperature profiles can now be constructed with the help of seismic reflection data using full waveform inversion [*Wood et al.*, 2008]. In another example, *Huang et al.* [2011] inverted for temperature and salinity distributions in sea water with depth from seismic data. The shallow part of the sea is poorly imaged because of few seismic traces for the shallow reflectors in the offset domain as well as due to the interference with the direct arrivals. *Han et al.* [2012] assumed soundspeed close to the sea-surface between 0 and 300 m as ~1500 m/s to estimate its variation with depth and illustrated its impact on reflection seismic imaging. However, direct arrival information can be used to fill in a knowledge "gap" between sea surface temperature data from the upper few meters of the water column and seismic oceanographic images of the water from the depths of a few hundred meters.

In the present study, we evaluate marine multi-channel seismic experiments for their potential to estimate sea surface temperature (SST). SST is an important oceanographic parameter as it governs the heat transfer between the ocean and the atmosphere [*Sura and Sardeshmukh,* 2008]. SSTs are used as a boundary condition for various atmospheric/weather simulation models. Historical knowledge of SST is required to understand the present day changes in the ocean and the atmosphere. The Intergovernmental Panel on Climate Change (IPCC) has shown that the increase in global SST by 0.4^{o}C from 1970 to 2000 leads to global warming [*Houghton et al.*, 2001]. Historical SST variation (MOHSST; *Parker et al.* [1995]) has been compiled from ship-based SST observations during the World Meteorological Organization (WMO) Voluntary Observing Ship (VOS) program. However, the range of observational methods used during the VOS program led to systematic bias in the SST values which needs to be corrected for reliable interpretation of climate change [*Kent and Taylor,* 2006]. Usually, SSTs are measured using ships or buoys. In the past two decades, satellites have been introduced to measure SSTs (e.g. *Wu et al.* [1999]). However, due to the skin effect, sea surface temperatures as measured by satellites can be very different from temperatures a few centimeters below the sea surface (i.e. in-situ temperatures) [*Emery et al.,* 1994]. Therefore, these satellite images in different radiation bands are calibrated with the in-situ temperature measurements at various locations [*Emery et al.*, 2001]. Such images have a great advantage as they provide uniform coverage with a high spatial resolution of ~1 km. The temperatures derived from marine seismic experiments are in-situ temperatures and can potentially

be used to study historical variations as they cover a limited time-period and to calibrate satellite-derived SSTs.

Marine multi-channel seismic experiments have been conducted along continental margins and oceanic basin for studies related to oil and gas exploration and structural and tectonic evaluations since the 1930s. The experiments consist of a seismic source, usually an airgun, which generates an impulsive energy pulse and a series of receivers, usually hydrophones, which receive the energy. The pressure wave that travels directly from source to receiver is known as the direct wave, and the waves reflected from the seabed and other subsurface structures are known as reflections. Conventional seismic processing ignores or removes the direct wave as it has little or no influence on subsurface structural imaging. However, the arrival time of the direct wave depends on the soundspeed of seawater.

Although, the processing of the direct waves in marine seismic data does not provide any useful subsurface information for oil and gas studies, method used for estimating soundspeed from direct arrivals are well established as they are used for static corrections in land seismic data processing [e.g., *Lawton*, 1989]. The two established methods are based on: 1) first break picks associated with direct arrivals, and 2) estimating the time delay of direct arrivals between adjacent receivers using cross correlations techniques. In marine seismic data, the application of these methods will yield the soundspeed near the sea surface, which then can be interpreted in terms of sea surface temperatures. We also present a novel approach that can be used to improve the signal-to-noise ratio prior to application of these methods using a wavelet-based, amplitude balancing technique [*Sinha*, 2014]. We have demonstrated the applicability of the methods for estimating sea surface temperatures using available multi-channel seismic data from the offshore Krishna-Godavari Basin (Figure 1) [*Dewangan et al.*, 2011]. The estimated soundspeeds from both the approaches, namely first break picking and cross-correlation, show comparable results. The result shows very high surface water velocities of ~1545 m/s with significant variations. The soundspeeds can be inverted to estimate the temperatures which are verified using the available CTD data in the study area acquired during the same month. Estimates of temperature are also consistent with the published temperature and salinity data from the North Indian Ocean Atlas (NIOA) [*Chatterjee et al.*, 2012]. In addition, temperatures estimated during different periods show diurnal variation.

THEORY AND METHOD

The speed of sound in sea water is governed by temperature (T), depth (D) (or pressure) and salinity (S). Empirical relationships developed by *Mackenzie* [1981][Equation (1)] and *Coppens* [1981] [Equation (2)] representing speed (c) in terms of these variables are widely used in oceanography.

$$\begin{aligned} c(T,D,S) = {} & 1448.96 + 4.591\,T - 5.304\,x\,10^{-2}\,T^2 + 2.374\,x\,10^{-4}\,T^3 \\ & + 1.340\,(S-35) + 1.630\,x\,10^{-2}\,D + 1.675\,x\,10^{-7}\,D^2 \\ & - 1.025\,x\,10^{2}\,T\,(S-35) - 7.139\,x\,10^{-13}\,T\,D^3 \end{aligned} \quad (1)$$

$$c(T,D,S) = c(T,0,S) + [1.6x10^{-6} + 2x10^{-8}(S-35)](S-35)T\,D + (1.623x10^{-2} + 2.53x10^{-5}\,T)D + (2.13x10^{-7} - 1x10^{-8}\,T)D^2$$

$$c(T,0,S) = 1449.05 + 4.57\,T - 5.21x10^{-2}\,T^2 + 2.3x10^{-4}\,T^3 + (1.333 - 1.26x10^{-2}\,T + 9x10^{-5}\,T^2)(S-35) \quad (2)$$

where temperature is in degrees Celsius, salinity is in PSU, depth is in meters and soundspeed is in m/s. Other competing equations and algorithms are also reported in the literature [*Chen and Millero*, 1977; *Fofonoff and Millard Jr.*, 1983; *Grosso*, 1974; *Wong and Zhu*, 1995], but we choose to use the Coppens equation because of its simplicity and the higher range of temperatures over which it is valid. The sensitivity of soundspeed $c(T,0,S)$ at the sea surface $(D=0)$ is analyzed by differentiating equation ((2) with respect to temperature and salinity as follows:

$$\frac{dc}{dT} = 4.57 - 0.1042\,T + 6.9x10^{-4}\,T^2 + (S-35)(-1.26x10^{-2} + 1.8x10^{-4}\,T) \quad (3)$$

$$\frac{dc}{dS} = 1.333 - 1.26\,x\,10^{-2}\,T + 9\,x\,10^{-5}\,T^2 \quad (4)$$

Taking the mean value of temperature and salinity from Table 2 as reference (i.e. 29.9^{o}C and 33.64 PSU), $\frac{dc}{dT}$ and $\frac{dc}{dS}$ are calculated to be 2.065 and 1.036, respectively. The sensitivity analysis shows that the soundspeed is twice as sensitive to temperature as it is to salinity [*Mamayev*, 2010]. Furthermore, large diurnal variations in sea surface temperature (up to 5^{o}C) are expected during calm periods when the surface wind is weak and insolation is strong [*Anderson and Riser*, 2014; *Kawai and Wada*, 2007]. Rapid fluctuation in sea surface salinity is expected during periods of strong currents and heavy precipitation. The seismic lines used in the present study were acquired over a short period of time [Table 1] and during a calm period. It is likely that the variation in soundspeed is predominantly due to variation in sea surface temperature rather than salinity. Therefore, the soundspeeds are inverted only for temperatures, while ignoring variation in salinity.

The speed of sound in seawater can be estimated by taking the ratio between the source-receiver distance (referred to as offset) and the arrival time of the direct wave. Some of the established seismic techniques for the estimation of soundspeed are the first break method and the cross-correlation method. The first break method, a conventional technique, is used for estimating soundspeed and static corrections during land seismic data processing. The methods for picking first breaks rely on seismic attributes such as energy ratio, fractal dimension, and entropy. Using a combination of statistical tests, *Hatherly* [1982] proposed to identify the first breaks. One of the challenges is to automatically estimate the arrival times of the direct wave from a shot gather; several methods have been developed for automated picking of the first arrivals. The method proposed by *Coppens* [1985] works well for high signal-to-noise ratio (S/N) data. Alternatively, the method proposed by *Spagnolini* [1991] used adaptive picking for the first breaks. The performance of the method degrades with a decrease in S/N. In order to improve the performance, *Sabbione and Velis* [2010] applied an edge preserving smoothness filter [*Luo et al.*, 2002] on shot gathers to pick rapid changes in seismic attributes near the first breaks.

Peraldi and Clement [1972] developed the method based on cross correlation to find the time delay (or lag) between direct arrivals in adjacent traces. The method is robust and works well for noisy data under the assumption that the source wavelet does not change between traces. *Gelchinsky and Shtivelman* [1983] constrained correlation properties by a statistical criterion to estimate speed from direct arrivals. The method lacks a zero time estimate and therefore, is not commonly used for static corrections. However, statistically this could be considered as a robust method for the estimation of soundspeed since there would be (N-1) data points from N traces.

In the present study, we evaluated both methods (first break method and cross correlation technique) for estimating the soundspeed near the sea surface from a seismic shot gather. The first approach involves picking the first breaks associated with the direct arrivals on hydrophone records. A linear relationship is expected between the first break time picks and the offset, and the best fit slope gives the speed of sound in seawater. We used a freely available automatic first break picking algorithm *sufbpickw* in Seismic Unix (CWP/SU) for estimation of arrival times. The method modifies Coppens' algorithm, using the energy ratio between the short-term window and the long-term window. We implemented a robust mispick correcting procedure involving a linear regression of the first breaks. The success of the second method depends on the S/N ratio as well as the wavelet shape found in the traces. The S/N can be increased using wavelet-based amplitude balancing [*Sinha,* 2014]. The amplitude balancing is achieved in the time-scale (time-frequency) domain. A brief description of the method is provided in the Appendix. Note that appropriate parameterization is required in each of the methods.

SEISMIC DATA

The proposed methods are demonstrated for the offshore Krishna-Godavari (KG) Basin, on the eastern continental margin of India (Figure 1). The available 2D multi-channel seismic (MCS) lines (12 seismic lines each ~100 km long) were acquired by Oil and Natural Gas Commission Ltd. (ONGC) for gas hydrates exploration [*Dewangan et al.,* 2011] in the KG Basin. The data were acquired using 8x40 cu.in. airguns fired every 12.5 m with a 1.5 km long streamer (120 channels, 12.5 m channel interval), and recorded with a 1 ms sampling interval and a high-cut filter set at 500 Hz. All available 6687 shot gathers are used in the present study. Record length (4.0 s) was truncated to 0.6 s (i.e., to just below the seafloor) in the present study. A maximum offset of 700 m is used in the present study as the S/N for direct arrivals is high. Date and time of acquisition, range of shot points and shooting directions for the available seismic data are summarized in Table 1.

RESULTS

We applied the proposed methods (first break and cross-correlation techniques) to the available shot gathers. The raw shot gathers have unusually low frequency (0.25 Hz) noise (e.g. Figure 2a) is most likely related to ocean surface swell, which is removed using scale-based filtering in the wavelet transform domain [*Bekara et al.,* 2008; *Elboth and Hermansen,* 2009; *Sinha and Sain,* 2015]. One processed shot gather is shown in Figure 2b. First break picks using *sufbpickw* in Seismic Unix (CWP/SU) are shown in Figure 2c. The cross correlation technique requires a constant wavelet pulse at all offset. Without shaping the direct arrival pulses, one would not be able to cross-correlate far offset traces with near offset traces. One might consider implementing compensation for

geometrical spreading to increase amplitudes of distant direct arrivals, but this has potential to increase noise in the data. As discussed in the method section, spectral balancing with an in-built noise suppression technique is used in the time-frequency domain to enhance the S/N (see Appendix). The spectral shaping of the direct arrivals is an important process in computing the speed of sound in near surface seawater as well as in automating the entire processes of soundspeed estimation.

The representative shot gather, after spectral balancing, is shown in Figure 2d. The direct arrival signature has improved significantly and is now suitable for use with the cross-correlation technique to estimate soundspeed. In the algorithm, we also applied several guides such as correlation strength and bounds on lags in order to pick the right time-delay for any given pair of traces. Likewise, the first break method was also automated for the estimation of soundspeeds from nearly 6700 shot gathers. The estimated soundspeeds from one of the 2D lines are shown in Figure 3a and b using first breaks and cross-correlations, respectively, and are quantitatively characterized by mean and standard deviation as the statistical parameters. Mean and standard deviation for the soundspeed estimates using first breaks and cross-correlations are 1546.19 m/s and 3.91 m/s (Figure 3a), and 1543.62 m/s and 2.00 m/s (Figure 3b), respectively. Although cross-correlation has smaller deviation, there is a remarkable agreement of the estimates from the two different methods that confirms the robustness of the procedure for soundspeed estimations. Narrower error bars related to cross-correlation method could be attributed to increased number of time-distance pairs in the method.

The observed soundspeed for near-surface water is around ~1545 m/s, which is high as compared to an average water velocity of 1500 m/s, typically used for marine seismic data processing. The soundspeed derived using equation (2) for the nearest CTD data is shown in Figure 4. Interestingly, the soundspeed estimated from the analysis of direct arrivals matches with the soundspeed for the near surface seawater derived from the CTD data. The soundspeed distributions (viz. Figure 3a and b) is more symmetric for the cross-correlation technique suggesting that the estimated soundspeeds using this technique may be more reliable than those estimated from the first break method. Using the cross-correlation technique, soundspeeds are estimated for all twelve lines and are plotted with respect to the shot locations in Figure 5a. The statistical distribution of the estimated soundspeeds is shown in Figure 5b.

DISCUSSION AND CONCLUSIONS

Temperature and salinity of seawater influence soundspeed as described by equations (1) and (2). Therefore, inversion of soundspeed for both temperature and salinity is non-unique. The rapid fluctuation of soundspeed within a short period of time is likely to be due to temperature variations in a water mass. Therefore, temperature is estimated from soundspeed assuming constant salinity using Coppens equation [*Coppens*, 1981]. Table 2 summarizes the sea surface salinity data from the available CTD profiles in the study area during the months of April and May. It is important to note that the study area receives a substantial volume of fresh water from the Krishna and Godavari rivers. *Chatterjee et al.* [2012] published the monthly North Indian Ocean Anomaly (NIOA) maps for sea surface salinity (SSS) by filtering and smoothing the salinity data. Since the seismic data

were acquired in the month of May, an average salinity of 34.2 PSU from the SSS map is used for the calculations. An average soundspeed of 1545 m/s gives a sea surface temperature of 30.15^{o}C. Interestingly, the average sea surface temperature in the month of May is reported to be 30.25^{o}C from NIOA and WOA09 [*Chatterjee et al.*, 2012] and 29.75^{o}C from [*Jaswal et al.*, 2012], close to that calculated from the seismic data. Marine seismic data have been recorded in a remarkably consistent way over time, including the archiving of such vital information such as position and time of collection of the data in the headers. Therefore, the proposed method can be used to estimate SST variability over decades of legacy data. This historical record of SST provides an important input for the various climate modeling/prediction codes. Also, such temperature estimates from direct arrivals can serve as a boundary condition for seismic thermometry using reflections within the ocean.

We have also attempted to examine the variability of the estimated soundspeeds in terms of diurnal variation in SST as the shot gathers are collected at different times of the day. *Clayson and Bogdanoff* [2013] report that diurnal warming typically reaches maximum values of 3^{o}C, although very localized events may reach 7^{o}C to 8^{o}C. The temperature estimates for all shot point locations are shown in Figure 6. The navigation data (see Table 1) of Lines 50, 49 and 48 show that they were acquired on the same day (May 02, 2004) at ~6 AM, ~10 AM and ~2 PM, respectively. We observe a very good qualitative correlation between the time of acquisition of these three lines and their respective temperature estimates. Line 50 shows the minimum temperature of 27.5^{o}C at ~6 AM whereas Line 48 shows the maximum temperature of 31.5^{o}C at ~2 PM. Line 45 shows an intermediate temperature of 28.5^{o}C at ~ 8AM. The temperature estimate from Line 49 is close to that from Line 45 as it was acquired at similar time of day. The other 2D lines were acquired on different dates and times and they also appear to contain diurnal variations of temperature. The observed diurnal temperature variation is about 3^{o}C. The sparse nature of the current datasets does not allow us to quantitatively analyze for diurnal temperature variations. However, the proposed method should have the capability to establish quantitative relationship for a comprehensive seismic data. The historical seismic data available from the NOAA-National Centers for Environmental Information (NCEI: www.ngdc.noaa.gov/mgg), the academic seismic portal (ASP) at the University of Texas at Austin (www.it.utexas.edu/sdc), the marine geosciences data system (MGDS: www.marine-geo.org), the Euro seismic project (www.eu-seased.net) and oil companies may be used to build a historical SST record.

ACKNOWLEDGMENTS

We would like to thank Directors of NGRI, NIO and RGIPT for supporting this study. We thank K. Vishwanath and B.J.P Kumar, DGH for providing the seismic data used in the present study. The authors acknowledge the Indian Oceanographic Data Center (IODC), NIO for providing the CTD data. The anonymous reviewers and associate editor are acknowledged for providing constructive comments which have improved the quality of the manuscript. The work was performed at RGIPT under research collaboration with NGRI and NIO. This is NIO contribution no: ____.

APPENDIX

Sound waves in water attenuate due to spherical divergence and dispersion. Furthermore, direct arrivals on near offset receivers are most often affected by bubble pulses, making them difficult to pick with automated pickers. Therefore, wavelet shaping is performed to increase accuracy in time-delay estimations. Conventional time or frequency domain processing, steps such as automatic gain control (AGC) or predictive deconvolution, tend to amplify noise along with the signal. For non-stationary signal analysis, time-frequency variant operators are preferred for wavelet shaping. In this case, the wavelet transform is naturally suited because the wavelet adapts to the frequency content of the signal providing improved control over both resolution and stability. There is a redundancy of scale which is effectively exploited to control noise amplification while performing the inverse wavelet transform, thus giving a stable algorithm for spectral balancing.

Spectral Balancing in the Wavelet Transform Domain

A continuous wavelet transform is often used for time-frequency representation of a time domain signal. This is preferred over a Short-Time Fourier transform as it does not require a user specified window length and the analyzing wavelet adjusts itself to the frequency content in the signal to optimize the time-frequency resolution [*Sinha et al.*, 2005]. In order to balance the time-frequency content throughout the record length, a smoothed spectrum surface is generated. The original time-frequency spectrum is balanced with respect to the smooth surface [*Sinha*, 2014]. A brief description of the method follows.

The time scale spectrum for a signal $f(t)$ is obtained by taking the inner product of a family of wavelets $\psi_{\sigma,t}(t)$ with the signal.

$$F_W(\sigma,\tau) = \langle f(t), \psi_{\sigma,t}(t) = \int_{-\infty}^{\infty} f(t) \frac{1}{\sqrt{\sigma}} \psi\left(\frac{t-\tau}{\sigma}\right) dt \qquad \text{(A-I)}$$

where σ is the scale and $F_W(\sigma,\tau)$ is the time-scale map. The inverse of the above transform of the above exists when the analyzing wavelet satisfies the "admissibility condition" given by,

$$C_\psi = 2\pi \int_{-\infty}^{\infty} \frac{|\hat{\psi}(\omega)|^2}{\omega} d\omega < \infty . \qquad \text{(A-II)}$$

The function *f(t)* is reconstructed as,

$$f(t) = \frac{1}{C_\psi} \iint_{-\infty}^{\infty} F_W(\sigma,\tau) \psi\left(\frac{t-\tau}{\sigma}\right) \frac{d\sigma\, d\tau}{\sqrt{\sigma}\sigma^2} . \qquad \text{(A-III)}$$

Spectral balancing of the signal is achieved by modifying $F_W(\sigma,\tau)$ before applying equation (A-III) for the inverse continuous wavelet transform. Essentially, a time and frequency dependent operator is obtained by smoothing the power scalogram $|F_W(\sigma,\tau)|$. For this purpose, we have used a 2D Hamming filter to construct the operator. *Margrave et al.* [2011] discuss other ways to construct a time-frequency varying 2D filter for spectral enhancement. In this trace-by-trace processing algorithm, we have used the Morlet wavelet which is a commonly used wavelet in seismic data applications. The wavelet is essentially a plane wave modulated by a Gaussian window [*Morlet et al.*, 1982].

REFERENCES

Anderson, J. E., and S. C. Riser (2014), Near-surface variability of temperature and salinity in the near-tropical ocean: Observations from profiling floats, *Journal of Geophysical Research: Oceans*, *119*(11), 7433-7448.

Bekara, M., A. Ferreira, and M. v. d. Baan (2008), A statistical technique for high amplitude noise detection: Application to swell noise attenuation, in *SEG Technical Program Expanded Abstracts 2008*, edited, pp. 2601-2605.

Chatterjee, A., D. Shankar, S. S. C. Shenoi, G. V. Reddy, G. S. Michael, M. Ravichandran, V. V. Gopalkrishna, E. P. R. Rao, T. V. S. U. Bhaskar, and V. N. Sanjeevan (2012), A new atlas of temperature and salinity for the North Indian Ocean, *J. Earth Sys. Sci.*, *121*, 559--593.

Chen, C.-T., and F. J. Millero (1977), Speed of sound in seawater at high pressures, *J. Acoust. Soc. Am.*, *62*(5), 1129--1135.

Clayson, C. A., and A. S. Bogdanoff (2013), The effect of diurnal sea surface temperature warming on climatological Air–Sea fluxes, *J. Climate*, *26*, 2546--2556.

Coppens, A. B. (1981), Simple equations for the speed of sound in Neptunian waters, *J. Acoust. Soc. Am*, *56*(4), 1084--1091.

Coppens, F. (1985), First arrivals picking on common-offset trace collections for automatic estimation of static corrections, *Geophysical Prospecting*, *33*, 1212--1231.

Dewangan, P., G. Sriram, T. Ramprasad, M. V. Ramana, and P. Jaiswal (2011), Fault system and thermal regime in the vicinity of site NGHP-01-10, Krishna–Godavari basin, Bay of Bengal, *Marine and Petroleum Geology*, *28*(10), 1899--1914.

Dushaw, B. D., P. F. Worcester, B. D. Cornuelle, and B. M. Howe (1993), On equations for the speed of sound in sea water, *J. Acoust. Soc. Am.*, *93*(1), 255--275.

Elboth, T., and D. Hermansen (2009), Attenuation of noise in marine seismic data, in *SEG Technical Program Expanded Abstracts 2009*, edited, pp. 3312-3316, Society of Exploration Geophysicists.

Emery, W. J., D. J. Baldwin, P. Schluessel, and R. W. Reynolds (2001), Accuracy of in situ sea surface temperatures used to calibrate infrared satellite measurements, *J. Geophys. Res.*, *106*(C2), 2387--2405.

Emery, W. J., Y. Yu, G. A. Wick, P. Schluessel, and R. W. Reynolds (1994), Correcting infrared satellite estimates of sea surface temperature for atmospheric water vapor attenuation, *J. Geophys. Res.*, *99*(C3), 5219--5236.

Fofonoff, N. P., and R. C. Millard Jr. (1983), Algorithms for computation of fundamental properties of seawater.

Gelchinsky, B., and V. Shtivelman (1983), Automatic picking of first arrivals and parameterization of traveltime curves, *Geophysical Prospecting*, *31*, 915--928.

Grosso, V. A. D. (1974), New equation for the speed of sound in natural waters (with comparisons to other equations), *J. Acoust. Soc. Am.*, *56*(4), 1084--1091.

Han, F.-X., J.-G. Sun, and K. Wang (2012), The influence of sea water velocity variation on seismic traveltimes, ray paths, and amplitude, *Applied Geophysics*, *9*(3), 319--325.

Hatherly, P. (1982), A computer method for determining seismic first arrival times, *Geophysics*, *47*(10), 1431--1436.

Holbrook, W. S., P. Paramo, S. Pearse, and R. W. Schmitt (2003), Thermohaline fine structure in an oceanographic front from seismic reflection profiling, *Science*, *301*(5634), 821--824.

Houghton, J. T., Y. Ding, D. J. Griggs, M. Noguer, P. J. v. d. Linden, X. Dai, K. Maskell, and C. A. Johnson (2001), *Climate Change 2001:The Scientific Basis*, 892 pp., Cambridge University Press.

Huang, X.-H., H.-B. Song, L. M. Pinheiro, and Y. Bai (2011), Ocean temperature and salinity distributions inverted from combined reflection seismic and xbt data, *Chinese Journal of Geophysics*, *54*(3), 307--314.

Jaswal, A. K., V. Singh, and S. R. Bhambak (2012), Relationship between sea surface temperature and surface air temperature over Arabian Sea, Bay of Bengal and Indian Ocean, *J. Ind. Geophys. Union*, *16*(2), 41--53.

Jones, E. J. W. (1999), *Marine Geophysics*, University College London.

Kawai, Y., and A. Wada (2007), Diurnal sea surface temperature variation and its impact on the atmosphere and ocean: A review, *J Oceanogr*, *63*(5), 721-744.

Kent, E. C., and P. K. Taylor (2006), Toward Estimating Climatic Trends in SST. Part I: Methods of Measurement, *J. Atmos. Oceanic Technol.*, *23*(3), 464--475.

Lawton, D. C. (1989), Computation of refraction static corrections using first-break traveltime differences, *Geophysics*, *54*(10), 1289--1296.

Luo, Y., M. Marhoon, S. A. Dossary, and M. Alfaraj (2002), Edge-preserving smoothing and applications, *The Leading Edge*, *21*, 136--158.

Mackenzie, K. V. (1981), Nine-term equation for the sound speed in the oceans, *J. Acoust. Soc. Am.*, *70*(3), 807--812.

Mamayev, O. I. (2010), *Temperature-salinity analysis of world ocean waters*, Elsevier.

Margrave, G., M. Lamoureux, and D. Henley (2011), Gabor deconvolution: Estimating reflectivity by nonstationary deconvolution of seismic data, *Geophysics*, *76*(3), W15-W30.

Morlet, J., G. Arens, E. Fourgeau, and D. Glard (1982), Wave propagation and sampling theory—Part I: Complex signal and scattering in multilayered media, *GEOPHYSICS*, *47*(2), 203-221.

Parker, D. E., C. K. Folland, and M. Jackson (1995), Marine surface temperature: Observed variations and data requirements, *Climatic Change*, *31*(2-4), 559--600.

Peraldi, R., and A. Clement (1972), Digital processing of refraction data: Study of first arrivals, *Geophysical Prospecting*, *20*, 529--548.

Sabbione, J. I., and D. Velis (2010), Automatic first-breaks picking: New strategies and algorithms, *Geophysics*, *75*(4), V67--V76.

Sinha, S. (2014), Data driven Q-compensation using continuous wavelet transform, in *SEG International Exposition and 84th Annual Meeting*, edited by B. Birkelo, pp. 4381--4385, Society of Exploration Geophysicists, Denver, USA.

Sinha, S., and K. Sain (2015), Denoising of seismic data in wavelet transform domain, in *3rd South Asian Geosciences Conference & Exhibition*, edited, AAPG, New Delhi, INDIA.

Sinha, S., P. S. Routh, P. D. Anno, and J. P. Castagna (2005), Spectral decomposition of seismic data with continuous-wavelet transform, *Geophysics*, *70*(6), P19--P25.

Spagnolini, U. (1991), Adaptive picking of refracted first arrivals, *Geophysical Prospecting*, *39*, 293--312.

Sura, P., and P. D. Sardeshmukh (2008), A Global View of Non-Gaussian SST Variability, *J. Phys. Oceanogr.*, *38*(3), 639--647.

Wong, G. S. K., and S. Zhu (1995), Speed of sound in seawater as a function of salinity, temperature and pressure, *J. Acoust. Soc. Am.*, *97*(3), 1732--1736.

Wood, W. T., W. S. Holbrook, M. K. Sen, and P. L. Stoffa (2008), Full waveform inversion of reflection seismic data for ocean temperature profiles, *Geophysical Research Letters*, *35*, L04608.

Worcester, P. F., et al. (1999), A Test of Basin-Scale Acoustic Thermometry Using a Large-Aperture Vertical Array at 3250-km Range in the Eastern North Pacic Ocean, *J. Acoust. Soc. Am.*, *105*, 3185--3201.

Wu, X., W. P. Menzel, and G. S. Wade (1999), Estimation of sea surface temperatures using GOES-8/9 radiance measurements, *Bull. Am. Meteorol. Soc.*, *80*, 1127--11138.

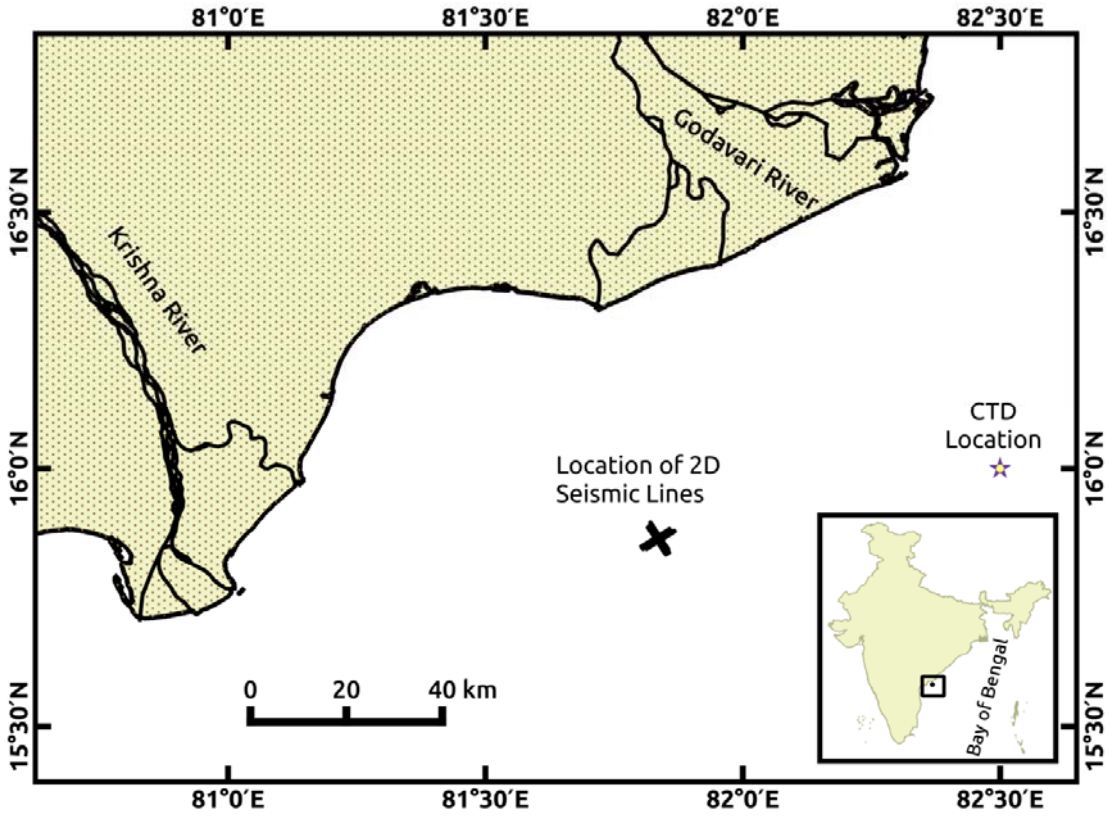

Figure 1: Twelve 2D-seismic lines were acquired in Krishna-Godavari Basin located in the eastern continental margin of India. Six lines are oriented in the NE-SW direction and the other six lines are oriented in NW-SE direction. The CTD location (star) is approximately 73 km from the seismic lines. The inset shows the zoom out map of the study location. There are two major rivers in the area: Krishna River and Godavari River.

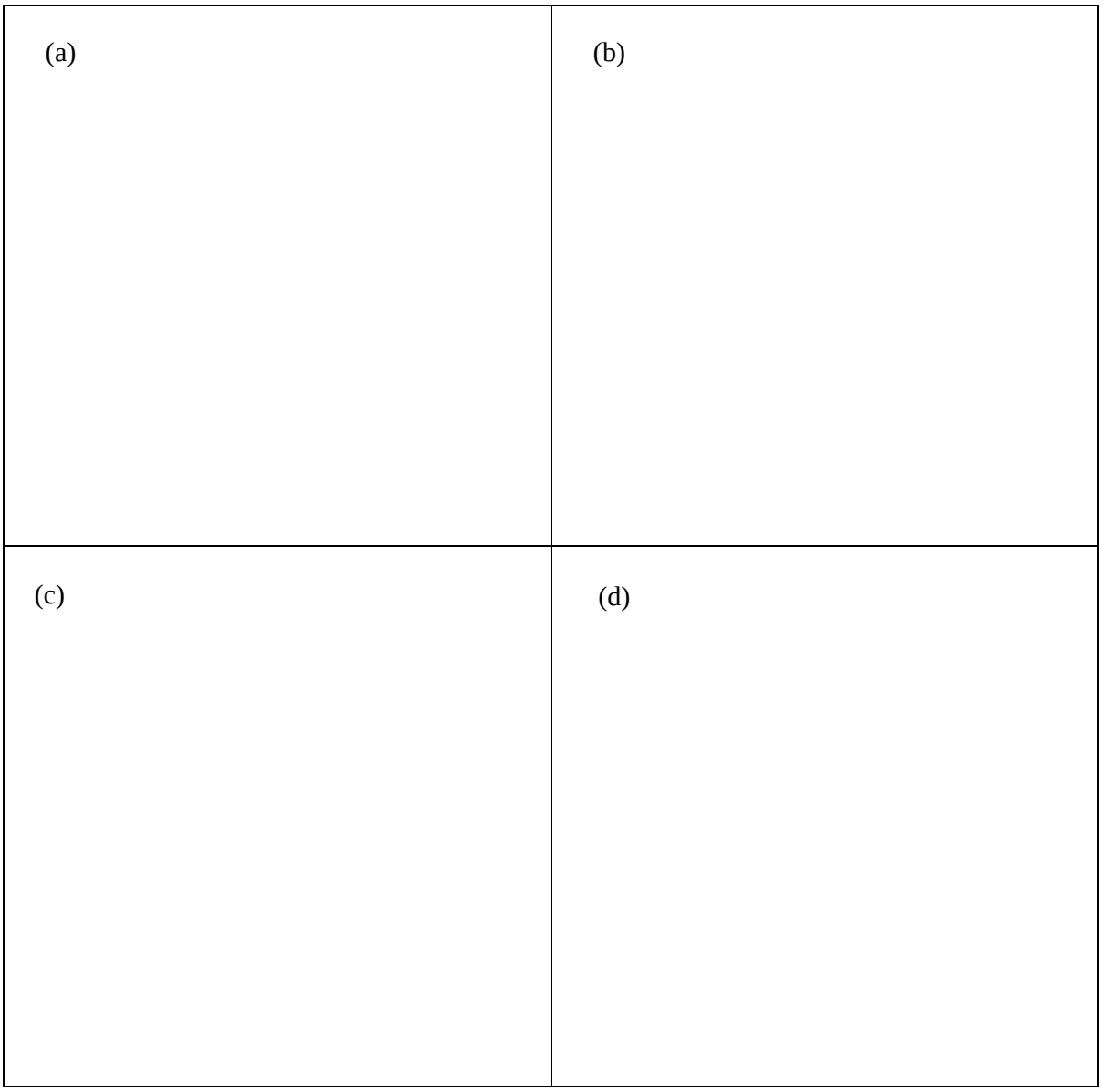

Figure 2: A representative shot gather (Line 50, SP No: 100) illustrating the processing steps involved in the first break picking. The raw shot gather is shown in (a). After removal of very low frequency noise, the gather is displayed in (b). Direct arrivals and first break picks are indicated by an arrow. The first breaks, picked using the Seismic Unix Program *sufbpickw,* are shown in (c). A white dashed line connects the maximum amplitudes on the first break picks. After spectral balancing, the shot gather is shown in (d) illustrating the enhancement in the direct arrival signals.

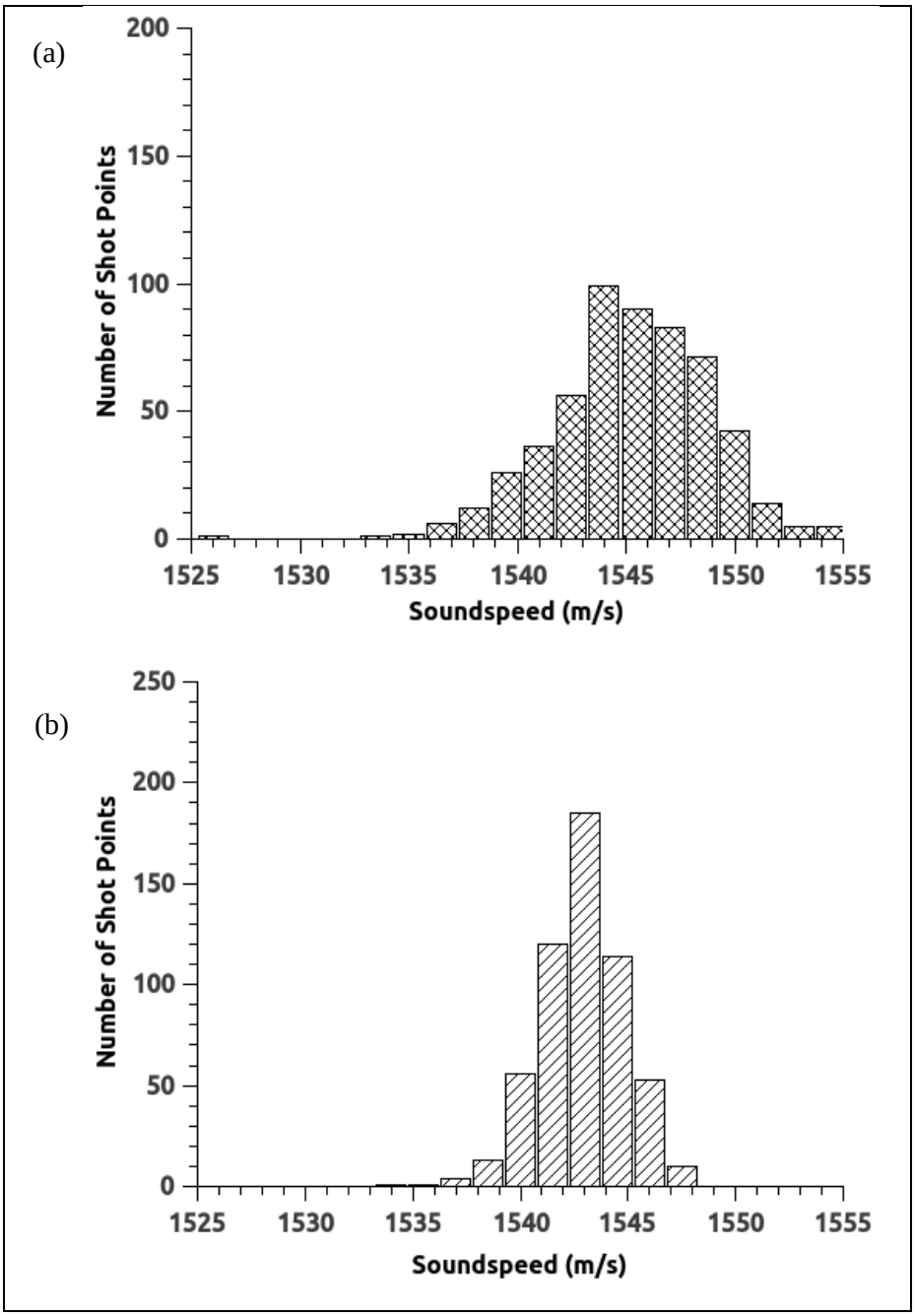

Figure 3: The statistical variation of soundspeeds in seawater computed for Line-14 using a) the first break method (Figure 2b) (mean: 1546.19 m/s and std dev: 3.91 m/s) and b) the cross-correlation technique on processed seismic data (Figure 2d) (mean: 1543.62 m/s and std dev: 2.00 m/s).

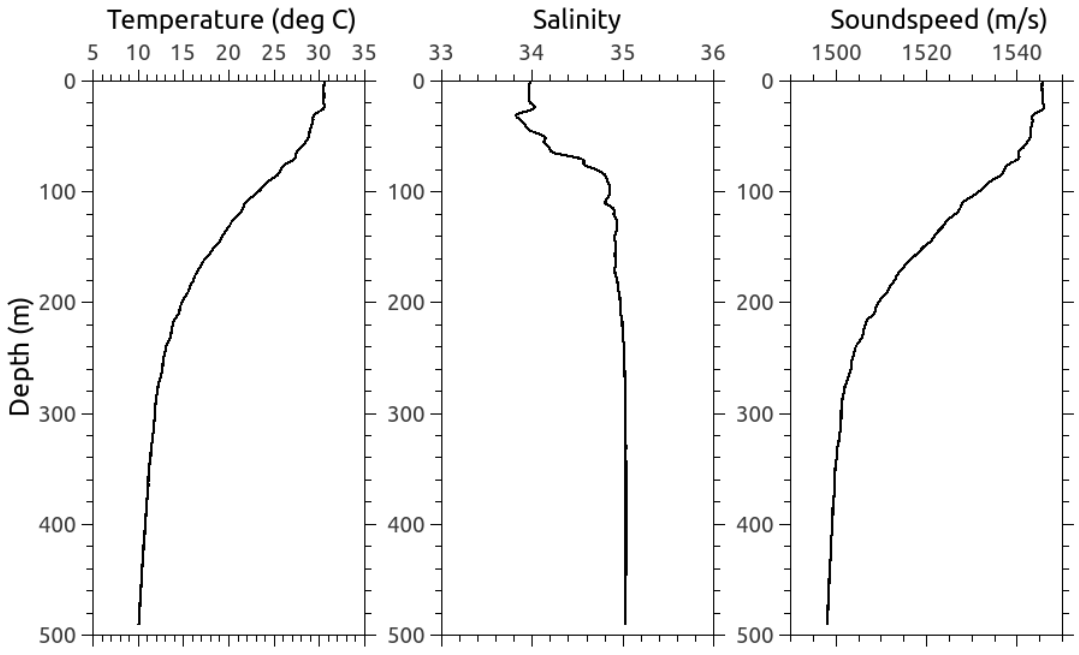

Figure 4: The variations in soundspeed computed using Coppens equation from the recorded temperature and salinity profiles at the CTD location shown in Figure 1. The data wer acquired on May 02, 2003 at 2:40 AM (Table 2).

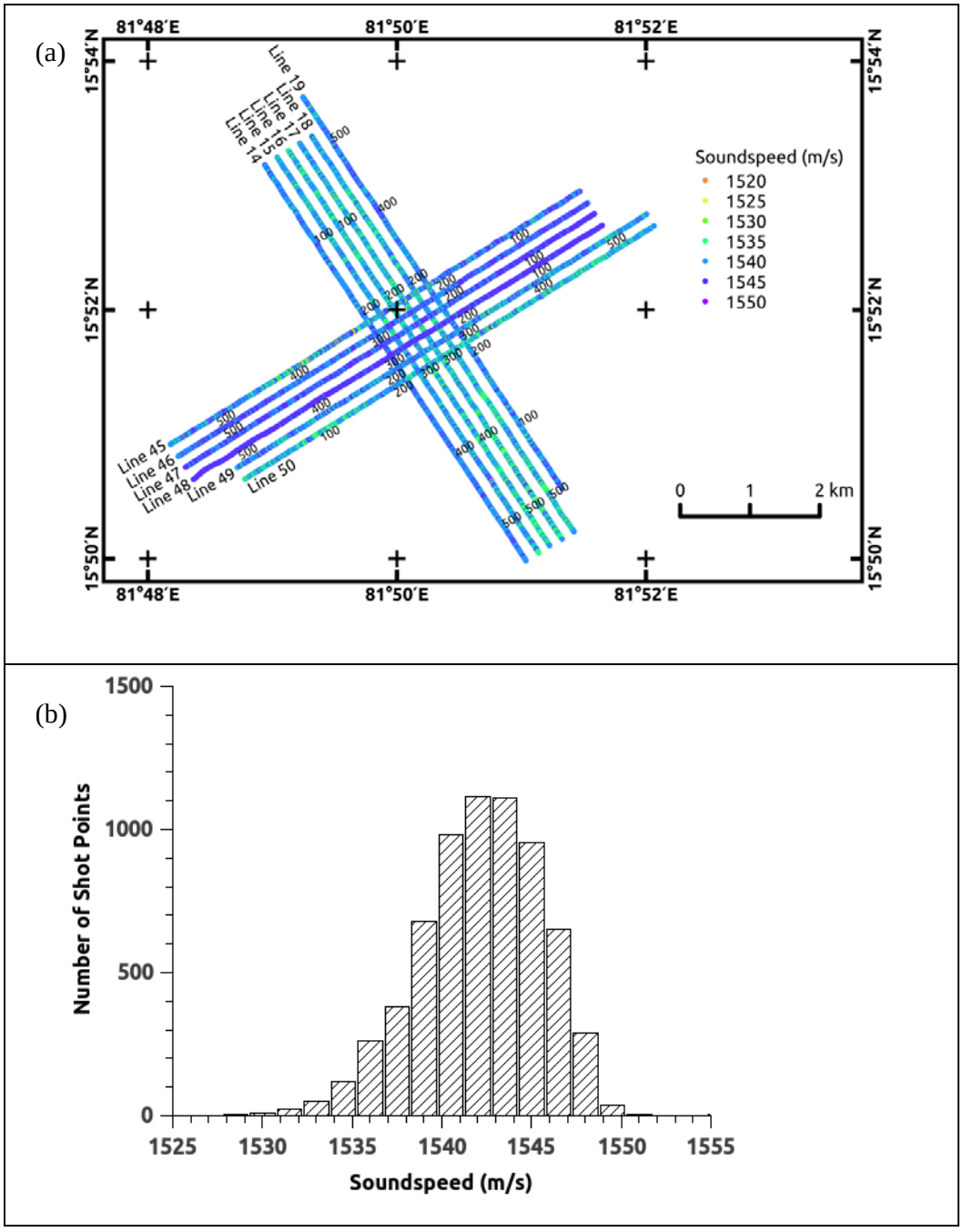

Figure 5: (a) The map view of the twelve 2D lines showing the locations of shot points are colored by respective soundspeed as estimated from the proposed cross correlation method. Line numbers are shown at one end and shot points are numbered at an interval of 100 along the lines. (b) Statistical distribution of soundspeeds for all lines /shots (Mean: 1542.89 m/s and std dev: 3.46 m/s).

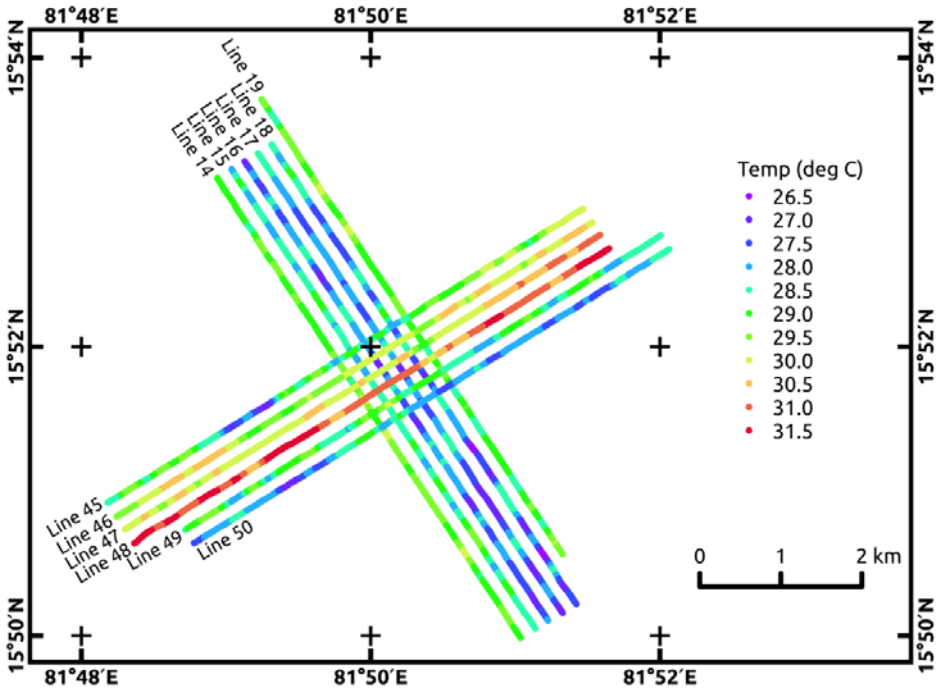

Figure 6: The estimated temperatures from soundspeed are plotted with different colors at respective shot locations for the available seismic data.

Line No.	Day of 2004	Time of Acquisition	Shot Point No
Line – 50	May 03	05:48 AM – 06:34 AM	1 (SW) – 558 (NE)
Line – 49	May 03	09:45 AM – 10:29 AM	1 (SW) – 558 (NE)
Line – 48	May 03	01:54 PM – 02:37 PM	1 (NE) – 558 (SW)
Line – 47	May 02	08:03PM – 08:49 PM (?)	1(NE) – 558 (SW)
Line – 46	May 02	08:03PM – 08:49 PM (?)	1(NE) – 558 (SW)
Line – 45	May 03	08:22 AM – 09:06 AM	1 (NE) – 558 (SW)
Line – 14	May 09	06:52 PM – 07:33 PM	1 (NW) – 557 (SE)
Line – 15	May 07	00:20 PM – 01:03 PM	1 (NW) – 557 (SE)
Line – 16	May 10	03:06 PM – 03:47 PM	1 (NW) – 557 (SE)
Line – 17	May 10	10:39 AM – 11:21 AM	1 (NW) – 558 (SE)
Line – 18	May 10	00:51 PM – 01:33 PM	1 (NW) – 558 (SE)
Line – 19	May 07	01:44 PM – 02:25 PM	1 (SE) – 552 (NW)

Table 1: Acquisition details from the navigation reports for the twelve lines are given in this table. Line numbers correspond to those shown on the maps (Figures 5a and 6). Duplicate date and time of acquisition for Lines 46 and 47 represents an error in the given navigation files.

Sl. No.	Latitude	Longitude	Date	Time	Temp. (deg C)	Salinity (PSU)	Distance (km)
1.	16° 00' N	82° 30' E	May 02, 2003	02:40 AM	30.47	33.96	73
2.	13° 00' N	81° 03' E	May 24, 1983	09:10 PM	30.56	33.45	328
3.	14° 00' N	81° 00' E	April 16, 1987	07:20 AM	29.32	33.19	225
4.	14° 00' N	81° 30' E	April 16, 1987	04:27 PM	29.86	33.78	210
5.	14° 00' N	82° 00' E	April 17, 1987	01:59 AM	29.47	33.56	207
6.	13° 58' N	81° 58' E	April 11, 1988	05:45 PM	30.52	34.31	211
7.	15° 00' N	81° 30' E	April 13, 1988	02:30 AM	30.08	33.9	102
8.	15° 00' N	81° 30' E	May 02, 2003	06:45 PM	30.49	33.92	102
9.	14° 00' N	81° 00' E	May 04, 2003	10:35 AM	29.80	34.23	225
10.	13° 00' N	81° 00' E	May 04, 2003	09:30 PM	30.22	33.99	330
11.	15° 00' N	81° 00' E	April 14, 2001	04:45 AM	29.01	32.90	131
12.	15° 00' N	82° 00' E	April 14, 2001	02:40 PM	29.19	32.50	97

Table 2: Available CTD data acquired in the months of April and May in the study area (source: Indian Oceanographic Data Center (IODC), NIO: www.nio.org/iodc/). The CTD locations, date and time of acquisition are listed. The surface temperature and salinity data of each CTD profile are also listed in columns 6 and 7. Distance of the CTD locations from the seismic lines are shown in the last column. Temperature and salinity profiles for the nearest CTD data (i.e. Sl. No. 1) are shown in Figure 4.